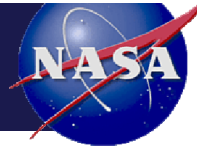
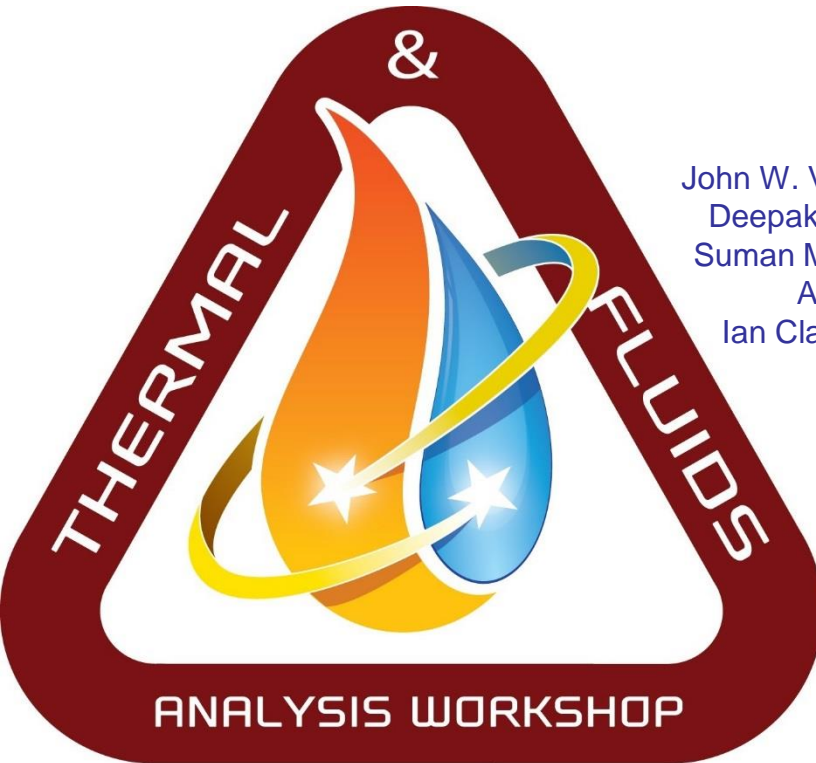


# TFAWS **Aerothermal** Paper Session



## PLUME INDUCED AERODYNAMIC AND HEATING MODELS FOR THE LOW DENSITY SUPERSONIC DECELERATOR TEST VEHICLE



Brandon L. Mobley – MSFC EV33 Aerosciences, Huntsville, AL

Sheldon D. Smith – MSFC EV33 – Jacobs, Huntsville, AL

John W. Van Norman – LaRC – Analytical Mechanics Associates, Inc., Hampton, VA

Deepak Bose – ARC - Analytical Mechanics Associates, Inc., Mountain View, CA

Suman Muppidi – ARC - Analytical Mechanics Associates, Inc., Mountain View, CA

A. J. Mastropietro – JPL/Caltech – Thermal Systems, Pasadena, CA

Ian Clark – JPL/Caltech – LDSD Program Principle Investigator, Pasadena, CA

Presented By:

Brandon L. Mobley

**TFAWS**  
MSFC • 2017

Thermal & Fluids Analysis Workshop  
TFAWS 2017

August 21-25, 2017

NASA Marshall Space Flight Center  
Huntsville, AL



# Agenda



- Background
- Analysis Objectives
- Approach
- Analyses
  - Spin Motor Plume Impingement Environments
  - Main SRM Plume Induced Environments
- Conclusions & Lessons Learned

- **LDSD Supersonic Flight Dynamics Tests (SFDT-1, 2)**
  - Test supersonic deceleration technologies in Earth's upper stratosphere, SFDT-1: June 28, 2014, SFDT-2: June 8, 2015
  - Balloon launched test vehicle, accelerated using a solid rocket motor (SRM) to achieve freestream test conditions (simulate Mars entry)
  - SFDT-1 & 2 Deceleration Technologies
    - Supersonic Inflatable Aerodynamic Decelerator - Robotic class (SIAD-R)
    - Parachute Deployment Device (PDD) – Ballute – Parachute extraction
    - Supersonic Disk Sail (SFDT-1) , Ring Sail (SFDT-2) Parachutes
- **Marshall Space Flight Center – EV33 Aerosciences - Roles**
  - Program onset - provide plume induced heating predictions throughout powered flight (main solid)
  - Spin motor plume impingement (heating and impact pressures)
  - Plume induced aerodynamics predictions (post-SFDT-1/pre-SFDT-2)

## Full Scale Testing in Earth's Stratosphere— Simulating Mars Entry

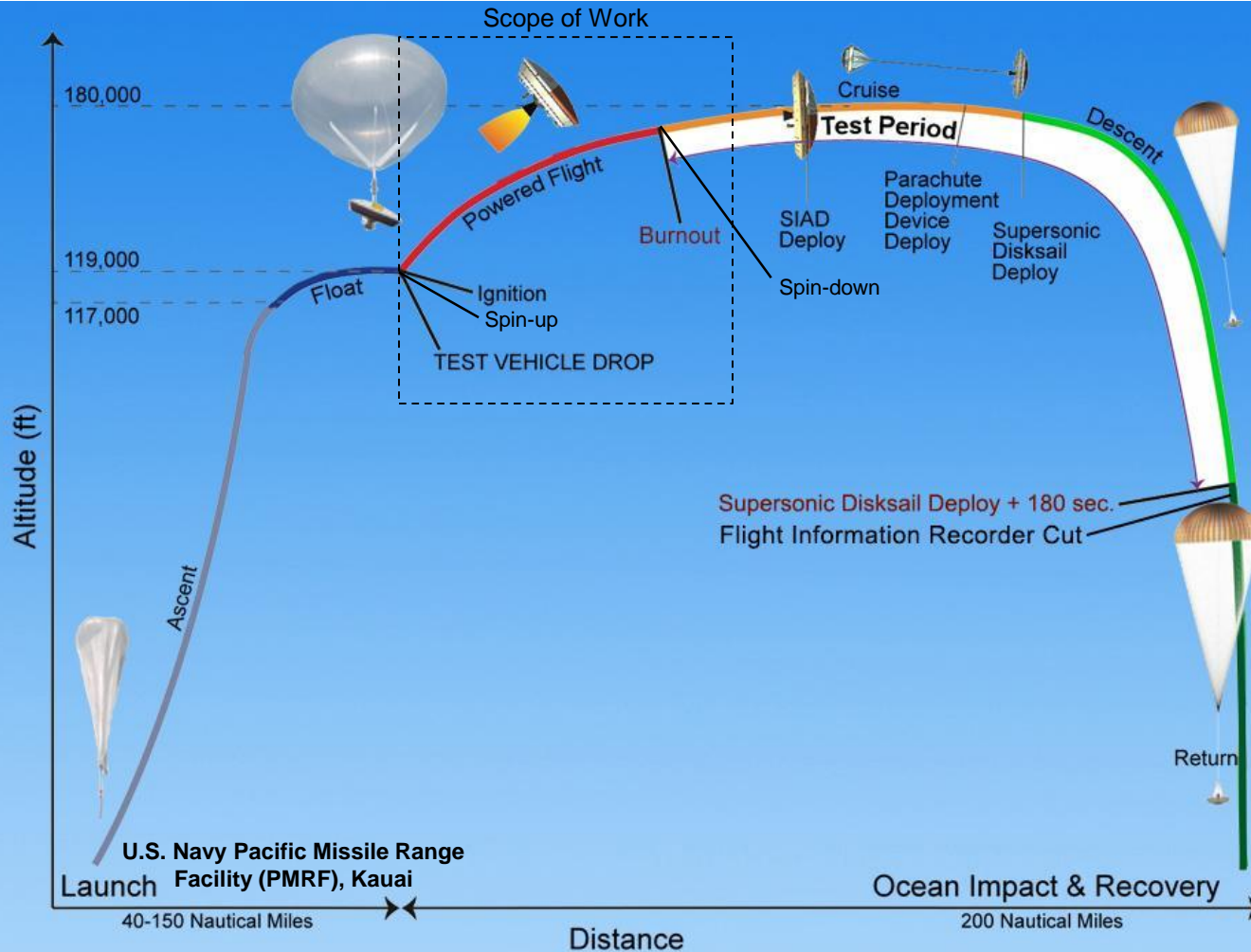
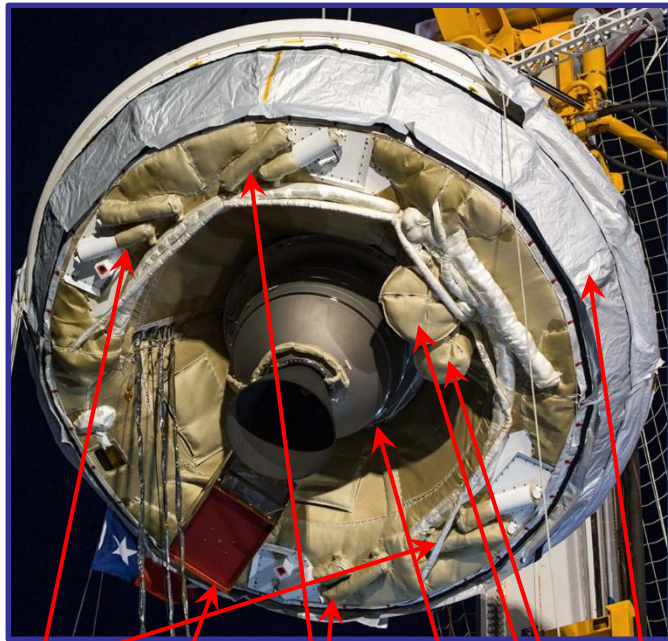
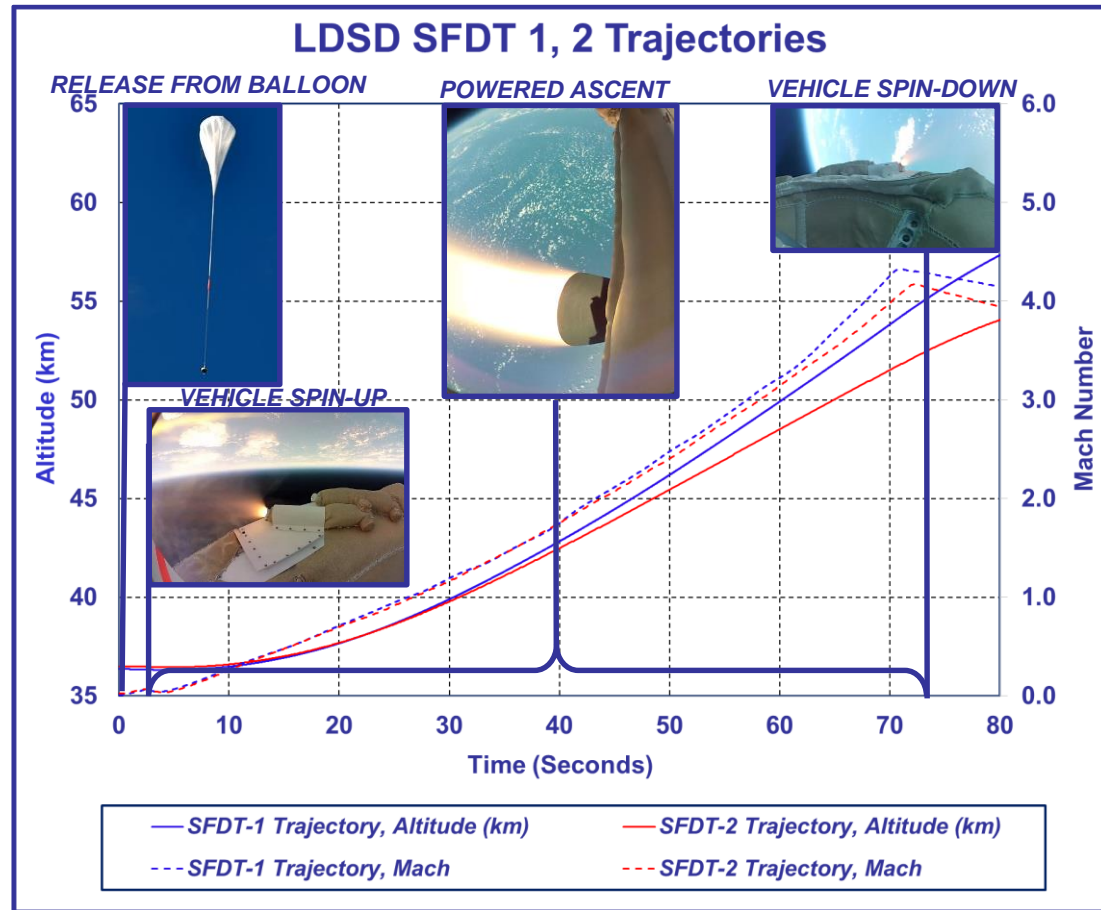


Figure Courtesy of JPL

- LDSD Test Vehicle and Trajectories (Best Equivalent)



**SPIN-UP MOTORS (2 PAIRS)**  
**SPIN-DOWN MOTORS (2 PAIRS)**  
**CAMERA MAST AND FLIGHT IMAGERY RECORDER**  
**MAIN SRM**  
**SIAD-R**  
**PDD**  
**SSRS**







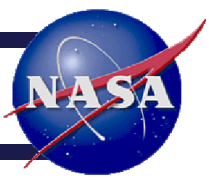
<b>Orbital-ATK Star-48B Long Nozzle Solid Rocket Motor</b>	
Expansion Ratio (A/A*)	54.8 (47.2 avg. nozzle erosion)
Throat Diameter	3.98 in / 10.11 cm
Exit Diameter	29.5 in / 74.93 cm
Nozzle Length	35.8 in / 90.93 cm
Chamber Pressure	Approximately 600 PSIA (@ t=0 sec)
Propellant (Approx. % Weight)	
71%	Ammonium Perchlorate
11%	Hydroxyl Terminated Polybutadiene (HTPB)
18%	Aluminum
Duration: Offloaded approx. 20% (400kg) to reduce burn time from 84 to 68 secs	



<b>Nammo Talley, Inc. Solid Rocket Spin Motor</b>			
Expansion Ratio (A/A*)	6.47		
Throat Diameter	0.86 in / 2.2 cm		
Exit Diameter	2.2 in / 5.59 cm		
Nozzle Length	1.82 in / 4.63 cm		
Chamber Pressure	Approximately 3057 PSIA (mean)		
Propellant (Approx. % Weight)			
83%	Ammonium Perchlorate	1.5%	Aluminum
9%	HTPB	1.5%	Fe <sub>2</sub> O <sub>3</sub>
5%	Plasticizer		
Duration: 0.25 secs			



# Analysis Objectives

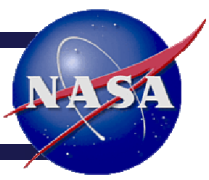


- 2012–2013 LDSD Thermal Design Support
  - Star 48 Plume Induced Base Heating
    - Radiation heat flux from  $\text{Al}_2\text{O}_3$  particles and plume gases
    - Convection from plume-air recirculation
  - Spin Motor Plume Impingement
    - Predict plume heating from convection and  $\text{Al}_2\text{O}_3$  particle impingement
    - Plume induced forces & moments (spin performance)
    - Primary concerns, impingement heating on SIAD, parachute bridles and mast cameras and instrumentation
- 2014–2015 Plume Induced Aerodynamics Support
  - Predict aerodynamic coefficients (forces & moments) during subsonic and transonic powered flight
  - Investigate plume flow field modeling sensitivities to aerodynamics

# Approach

- Simulate plumes throughout a flight trajectory at discrete points in time in a quasi-steady fashion
  - Two step approach, nozzle flows using engineering codes
  - Nozzle solutions used as boundary conditions to CFD domain
- Nozzle Flow Field
  - Model chamber and nozzle flow field chemistry using the NASA Glenn Chemical Equilibrium Combustion (CEC) program
  - Model two-phase nozzle flow, core and boundary layer, using the Reacting and Multiphase Program (RAMP2) & Boundary Layer Integral Matrix Procedure (BLIMPJ) engineering codes (MOC codes)
- CFD (induced forces and convection) - Loci-CHEM 3.3 p4
- Spin Motor Plume Particle Heating – PLIMP eng. code
- Plume Radiation (sep. series of plume solutions, Star 48)
  - RAMP2 – Gaseous and aluminum-oxide particle plume flow field
  - Reverse Monte Carlo – Particle, gaseous band model code





- **CFD Grid Challenges**

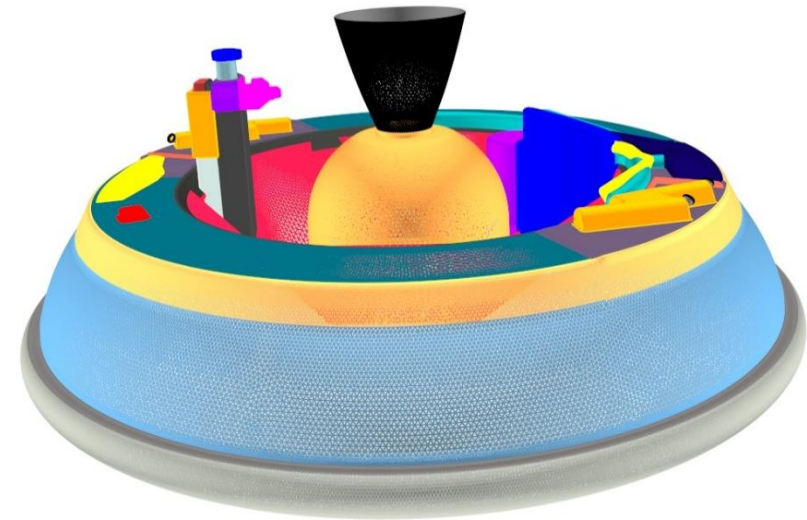
- Approach – Generally, try to create one grid to accommodate many cases, opposed to #grids refined for each case
- Variation of motor firing configurations (2, 4)
  - 1 spin-up and 1 spin-down grid to suit case
  - Tailored surface geometries per spin motor impingement, removed protuberances “behind motors”
- Variable angles of attack
- Subsonic / supersonic free stream conditions (shock refinement, aspiration refinement/convergence)

- **Grid Generation**

- ANSA 14, Solid Mesh 5.9.9 – Surface Grids, Volume Setup
- AFLR3 – Unstructured – Volume Grids

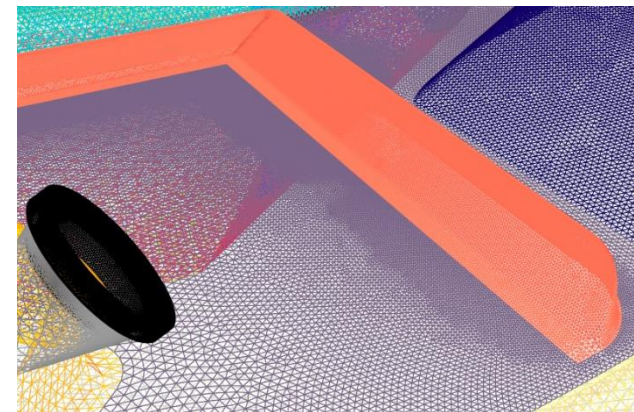
## Summary of CFD Settings, RANS

## Spin-Up Motor Surface Mesh (Final Iteration, 174M)



Category	Model Setup		
Case Description	Spin-Up Motors	Spin-Down Motors	Star48B Motor
Number of Plumes Simulated	4 (all on) and 2 (staggered firing)		1
Angle-of-Attack, $\alpha$ , and Side-Slip, $\beta$ , Angles	$\alpha = 163^\circ, \beta = 0^\circ$	$\alpha = 0^\circ, \beta = 0^\circ$	Various, per trajectory
Plume Chemistry	Frozen		
No. Species	2 - Equivalent air & plume gas		
Thermodynamic and Transport Properties	Thermally perfect gas, specie Cp varies with temperature, polynomial		
Specific Heat, Cp	Transport Fit (equivalent $\mu(T), k(T)$ , per specie)		
Viscosity and Conduction Models	Laminar-Schmidt		
Diffusion Model	Aluminum-Oxide		
Particle Model	None	Lagrangian (1 Case)	
Type		5, 1.662 - 4.557 $\mu$ m	
Number of Particle Bins & Sizes	Menter's Shear Stress Transport, SST		
Turbulence Model	Sarkar		
Compressibility Correction	0.10		
Urelax (m/s)	Varied per case, generally 0.001 - 0.0001 sec		
Dt Max (sec)	2nd Order, steady-state solutions		
Accuracy	No slip, vehicle spin rate applied		
Surface Boundary Conditions	Wall Temperatures		255 K
	255, 973, 1773 K		
	Vehicle Spin Rate	0	50 (RPM)
	Internal Nozzle Wall Thermal	Adiabatic Wall ( Carbon Phenolic)	
Solver	Guass-Seidel		

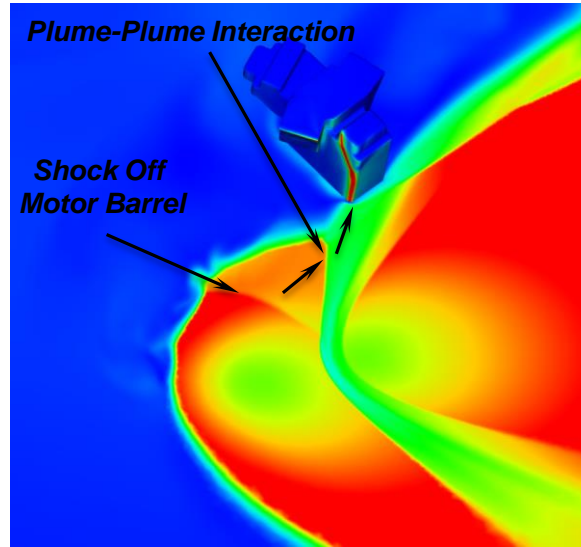
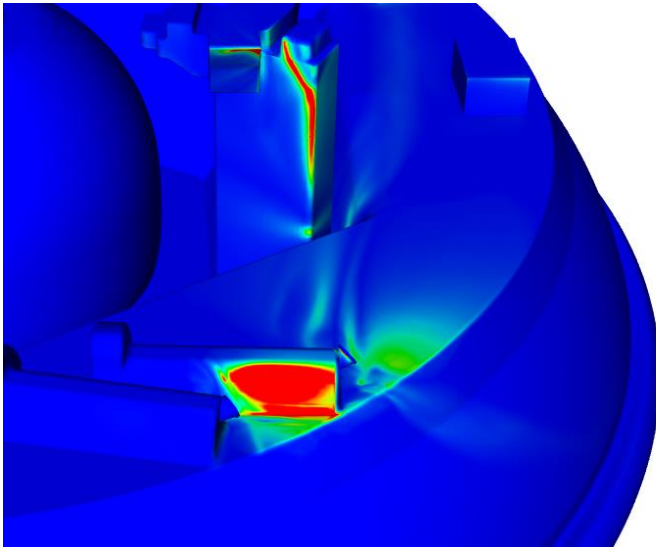
## STAR 48 SFDT-2 & Spin Motor Case Conditions



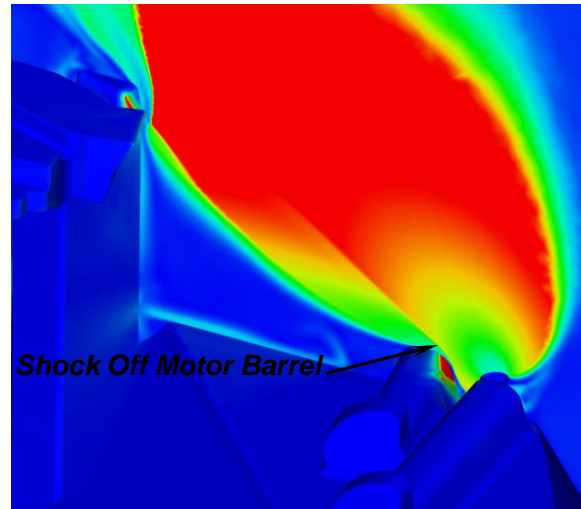
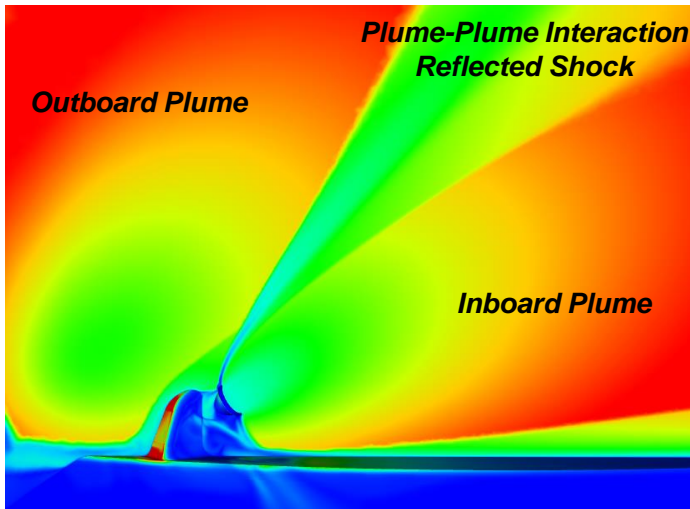
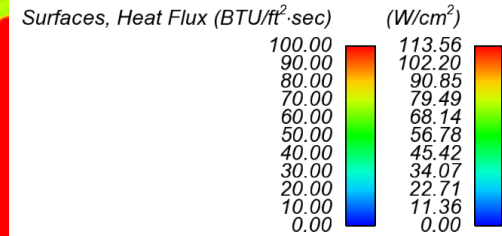
Trajectory Atmospheric Conditions					Chamber Conditions			Vehicle Attitude	Notes
Alt (km)	M <sub>∞</sub>	q <sub>∞</sub> (Pa)	P <sub>∞</sub> (Pa)	T <sub>∞</sub> (K)	Po (psia)	P <sub>tip</sub> (psia)	$\theta_{Press Exp Ratio}$	$\alpha_{Total}$ (deg)	
36.050	0.01	0.84	499.03	246.00	3057.00	70.10	968.52	163.0	SPIN MTR, PRE-SFDT-1
36.322	0.10	3.46	494.00	242.00	643.68	1.61	22.54	40.4	Post-SFDT-1, Star 48, ADB
36.390	0.20	13.71	489.69	241.88	643.68	1.61	22.74	30.0	Post-SFDT-1, Star 48, ADB
36.514	0.30	30.30	481.00	242.00	643.68	1.61	23.15	22.3	Post-SFDT-1, Star 48, ADB
36.993	0.50	78.75	450.00	244.00	606.29	1.57	24.01	17.7	Post-SFDT-1, Star 48, ADB
37.617	0.70	141.66	413.00	244.00	607.40	1.59	26.46	17.1	Post-SFDT-1, Star 48, ADB
38.449	0.90	208.66	368.00	246.00	607.40	1.59	29.70	14.7	Post-SFDT-1, Star 48, ADB
38.682	0.95	225.53	357.00	248.00	607.40	1.59	30.61	14.4	Post-SFDT-1, Star 48, ADB
39.469	1.10	271.04	320.00	253.00	616.23	1.68	36.17	12.7	Post-SFDT-1, Star 48, ADB
49.480	4.23	1171.60	93.10	266.96	3057.00	70.10	5191.44	0.0	SPIN MTR, PRE-SFDT-1

## INITIAL ANALYSIS

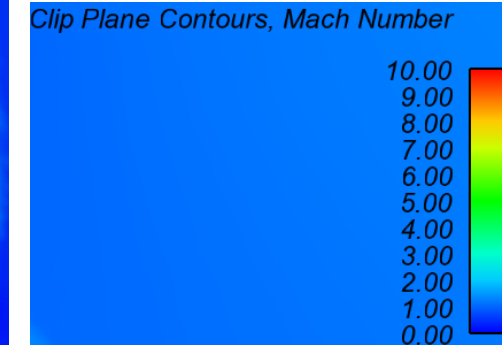
SPIN-UP – 120 Kft (36.6 km),  $P_\infty = 0.72$  PSIA (499 Pa) - ALL SPIN-UP MOTORS “ON”



### Surface Contours



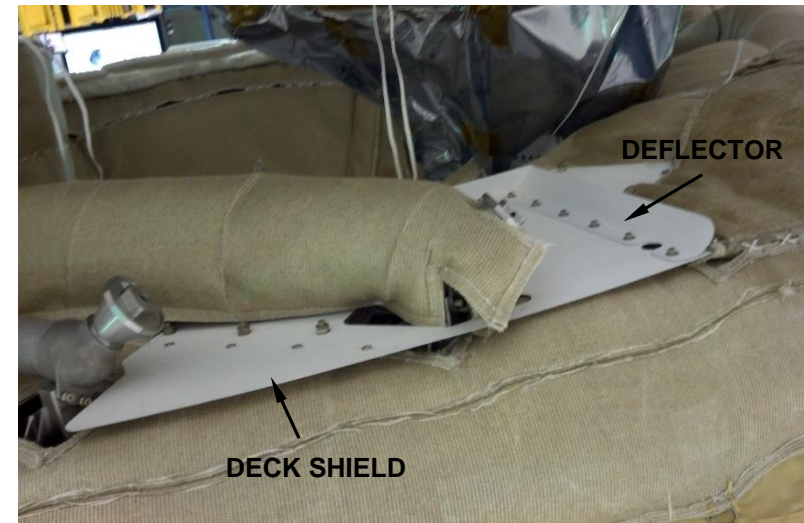
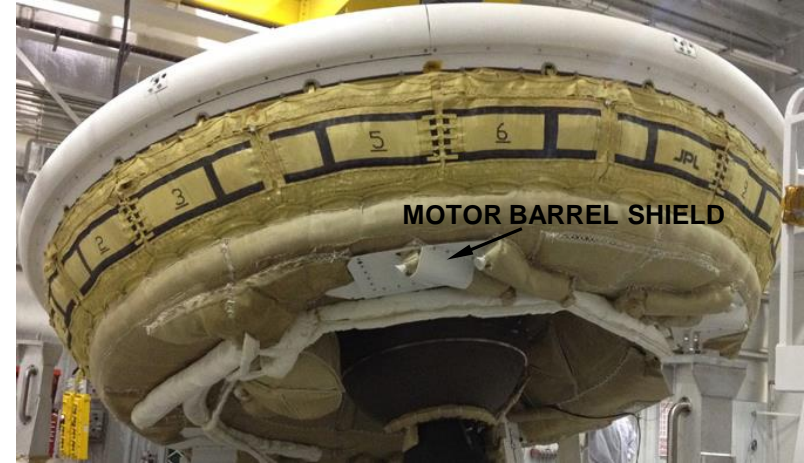
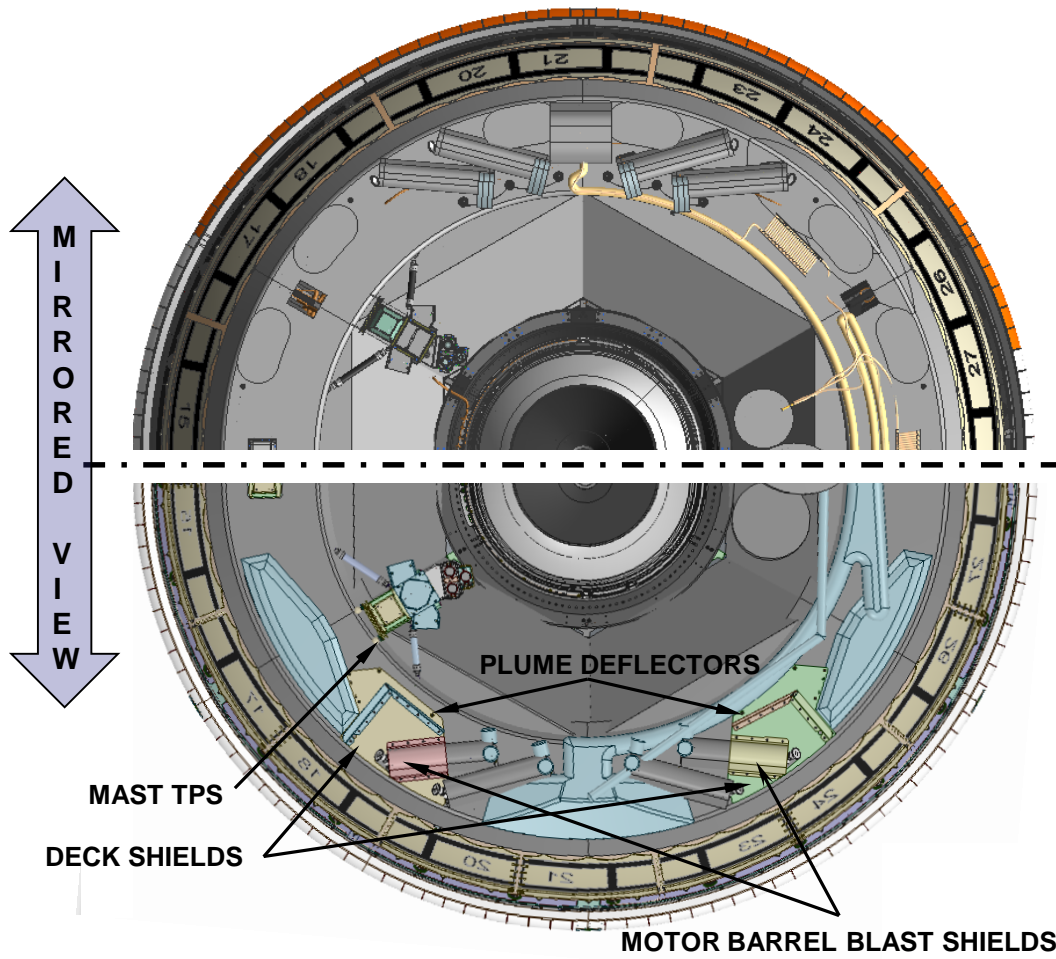
### Solution Plane Contours



- Initial Spin Motor Plume Impingement Summary
  - Motor casings, bridle coverings - severe heating areas, peak heat rates in excess of 500 BTU/ft<sup>2</sup>sec (568 W/cm<sup>2</sup>)
  - Camera mast, peak heat rates in excess of 200 BTU/ft<sup>2</sup>sec (170 W/cm<sup>2</sup>)
- Thermal and Operational Design Impacts
  - Two week “Tiger Team” to provide thermal protection options
  - Added plume deck blast shields, motor barrel shields and deflectors
    - Restricted height to prevent potential entanglement with chute brid. lines
  - Thermal protection (TPS) increased on camera mast (thin cork)
  - Staggered firing configurations (driven by flight dynamics, flight-ops as well)



BEFORE INITIAL PLUME ANALYSIS

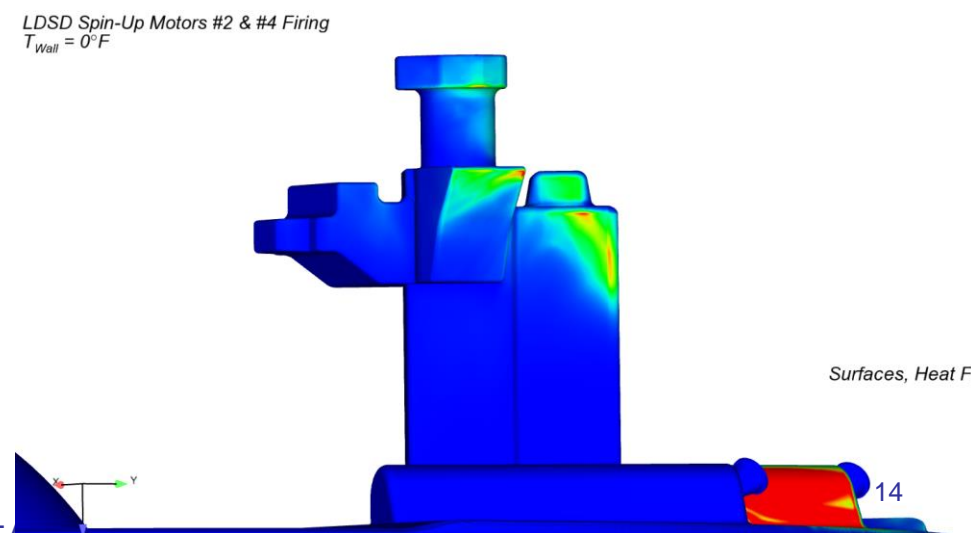
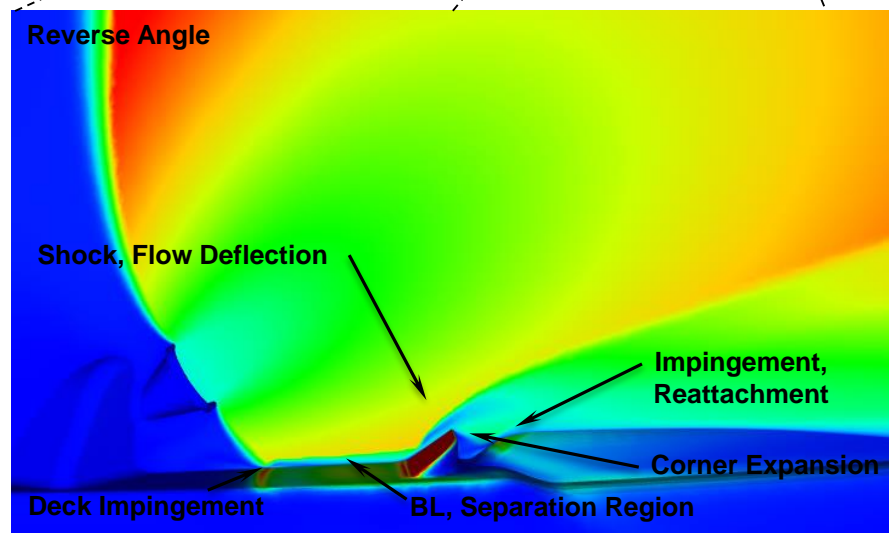
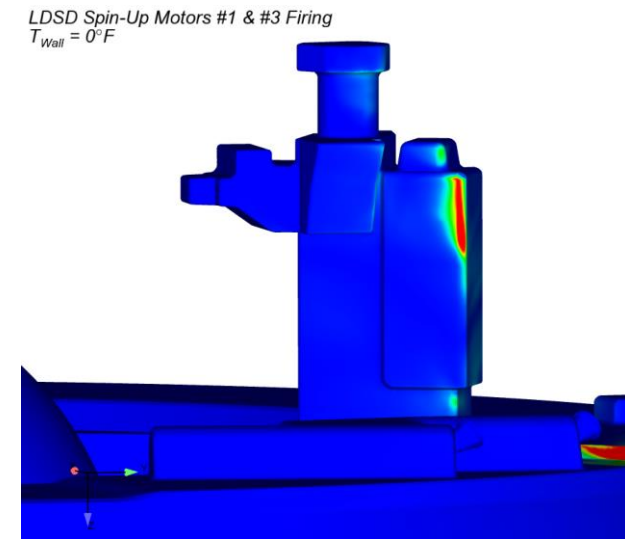
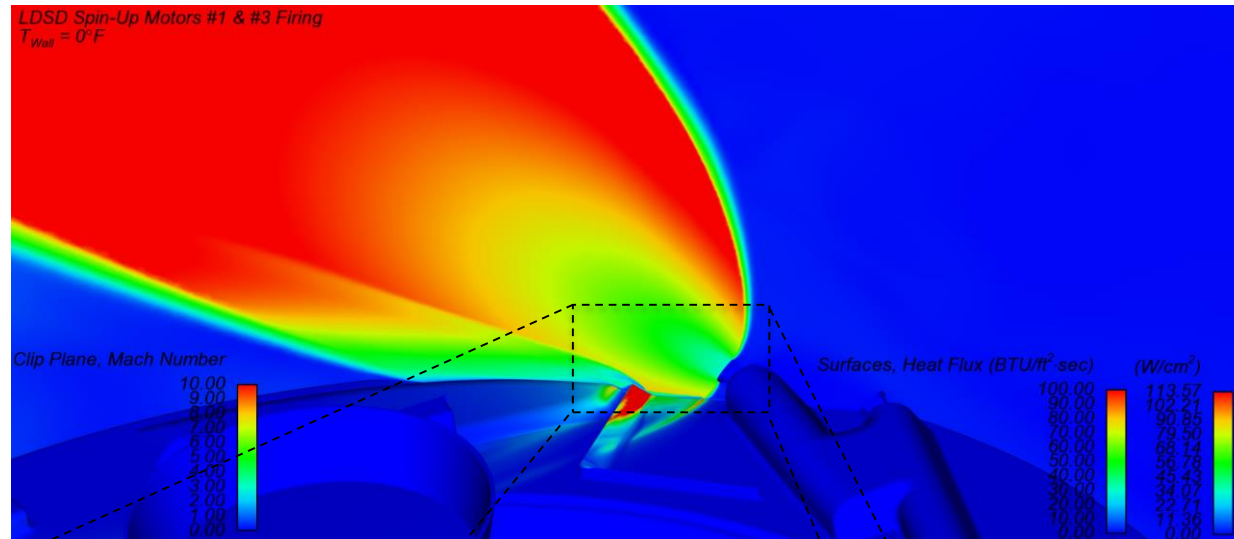


AFTER (MIRRORED PICTURE)



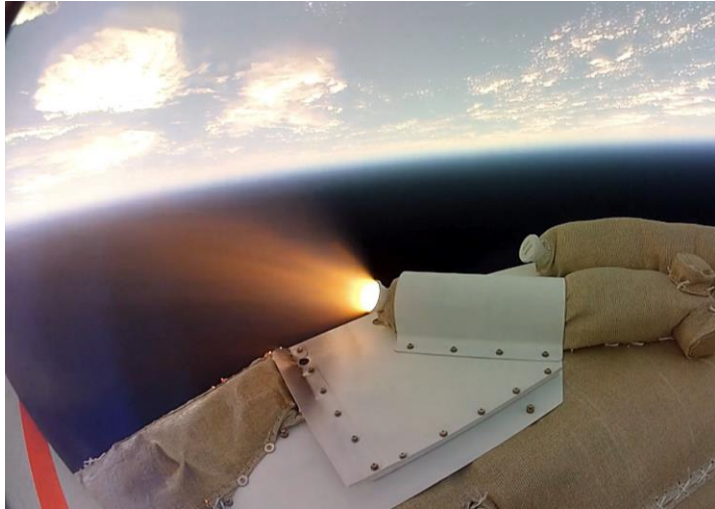
## FOLLOW-UP ANALYSIS

**SPIN-UP – 120 Kft (36.6 km),  $P_\infty = 0.72$  PSIA (499 Pa) – STAGGERED FIRINGS**

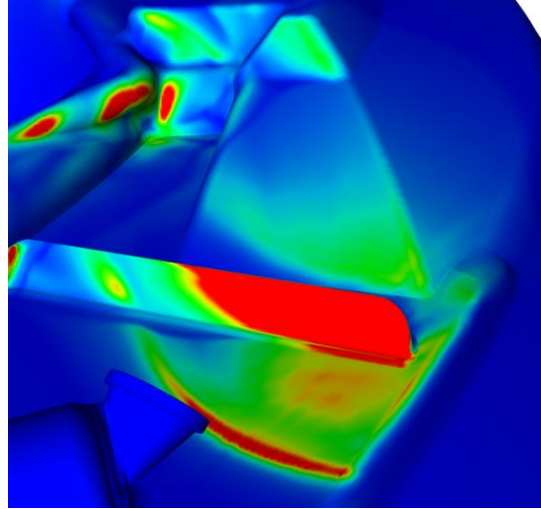


## SFDT-1 June 28, 2014

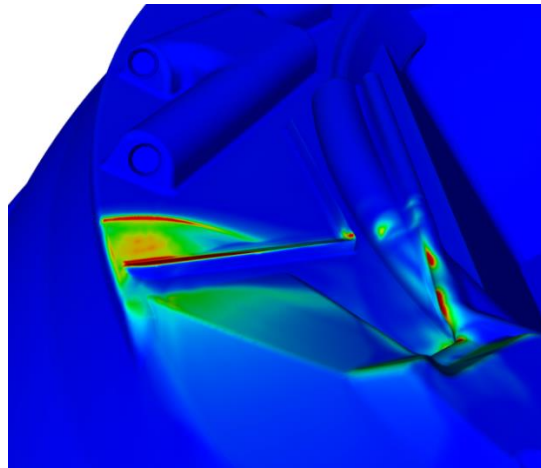
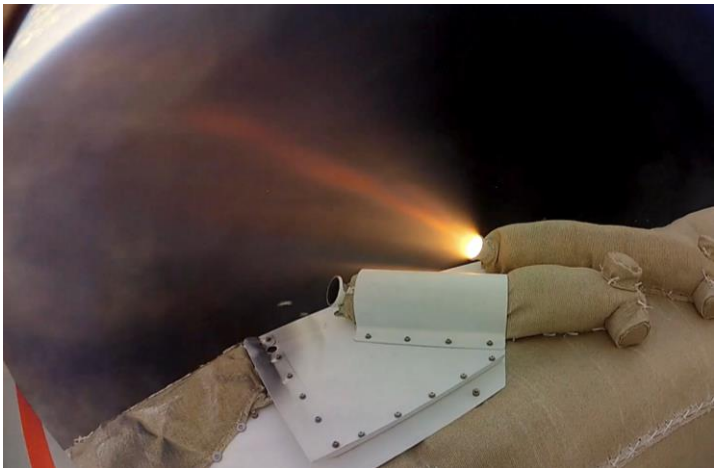
### Spin-Up Motor Firings



### Pre-flight Heating Contours

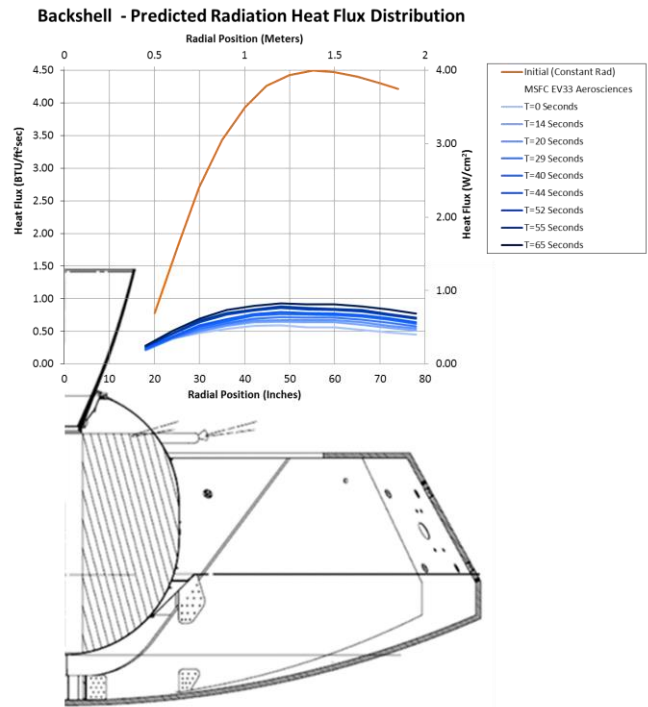
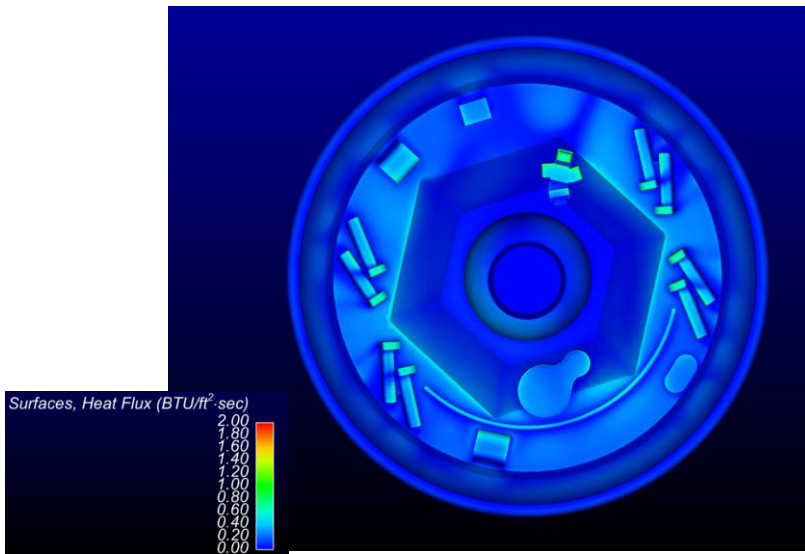


### Post-flight Charring



- Pre-SFDT-1 Star 48 plume induced heating environments
  - Predicted radiation rates approximately a factor of 4 less than initial
  - Predicted base pressure coefficient always negative, predicted convective heat rates generally  $< 1 \text{ BTU/ft}^2\text{sec}$
  - No thermal issues, **very benign**, highest temperatures were recorded on the Star 48 motor case (282 C, driven by internal environment)

Pre-SFDT-1 Convective Heating Prediction, 151Kft





- SFDT-1 flight reconstruction revealed the test vehicle over shot the targeted altitude approximately 10Kft
  - No chamber pressure measurements, no distinct way to accurately decoupling thrust and drag (challenge on determination of  $C_A$ )
  - Thrust reconstruction analysis revealed slightly over performing solid and over prediction of plume induced drag
  - Over predicted total moment (pitch-yaw) coefficient, resulting in the vehicle lofting more than expected

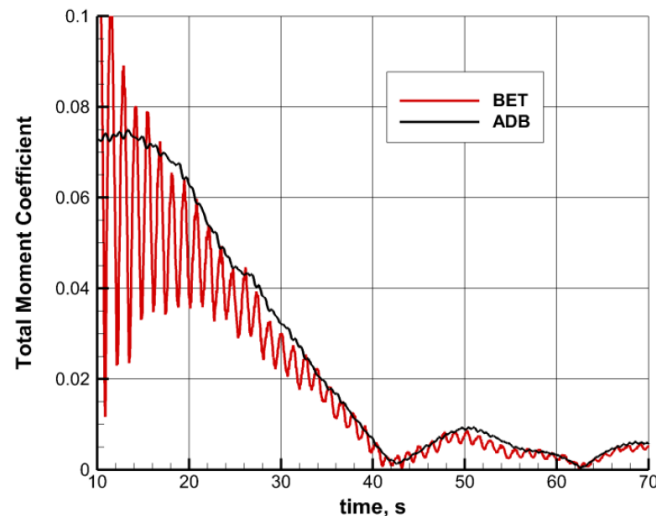


Figure Courtesy of John Van Norman, LaRC

- LDSD plume induced base flow field is different than “traditional” launch vehicles and missiles
  1. Blunt body - Realm of historical launch vehicles and missiles have a large slenderness ratio, where there is considerable running length to allow the development of a thick boundary layer that enters the base
  2. Ratio of base-to-nozzle exit area – free stream expansion angle entering the base, relative base eddy scale. Aft cavity provides recovery volume that affects the base environment
  3. Variation in total alpha due to spin/flight dynamics

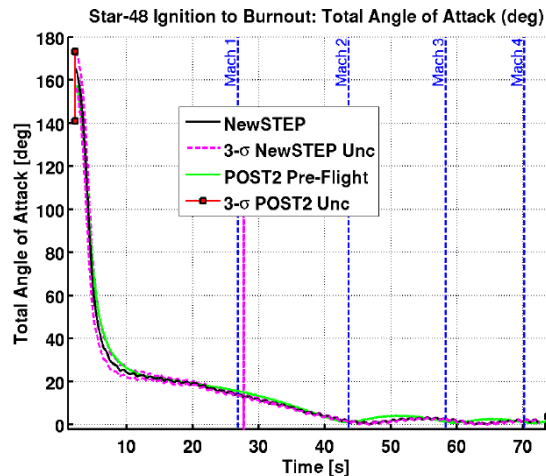
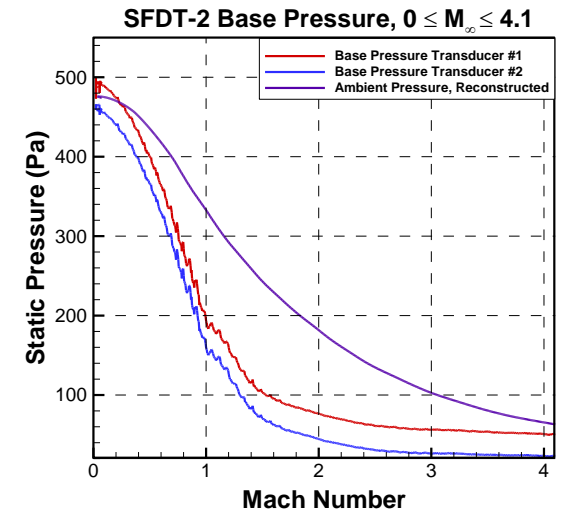
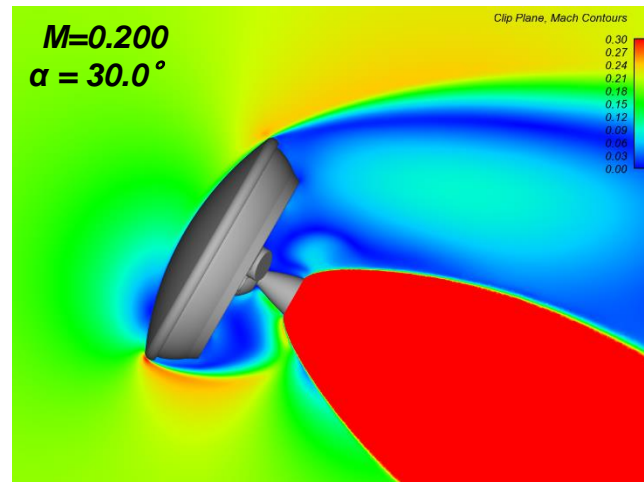


Figure Courtesy of Clara O'Farrell, JPL





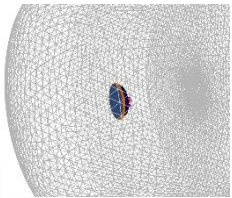
## Grid Evolution – Star 48

Initial Grids, Pre-SFDT-1 Heating (41 - 90 million cell, 2013)

*Predominantly supersonic cases,  $1.1 < M_\infty < 4.3$ , need higher  $q_\infty$  for recirculation*

*Simple geometry & trajectory ( $\alpha_{total}=0^\circ$ , small vol.  $O \sim 0.1 \text{ km}^3$ )*

*Primary objective, resolve forward shock, plume induced base recirc. (avg heating)*



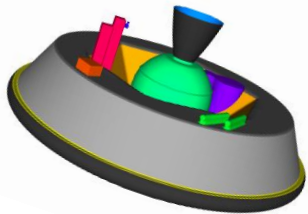
Post-SFDT-1 (90, 136 million, 2014 )

*Sub, transonic cases ( $M_\infty=0.5 - 1.2$ , “larger” vol.  $O \sim 1 \text{ km}^3$ )*

*Two geometries, reconstructed traj. subset ( $\alpha, \beta = 0, 10, 20^\circ$ )*

*Multiple Models – Plume w/wout particles, hybrid RANS/LES (423M)*

*Objective, predict plume induced aero. forces & moments*

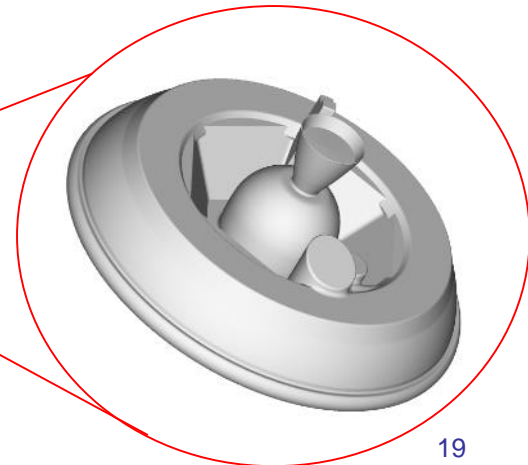
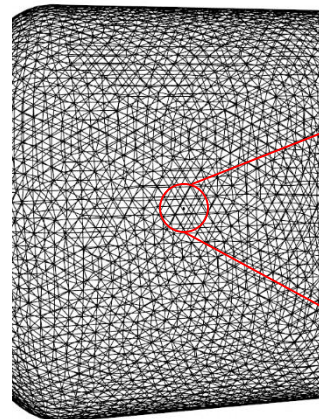
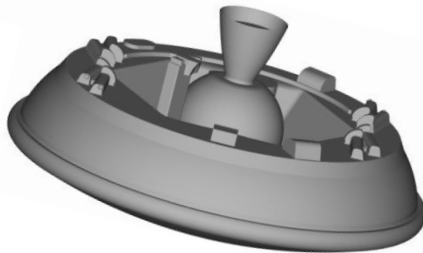


Pre-SFDT-2 (190 million, 2015 )

*Sub, transonic cases ( $M_\infty=0 - 1.2$  “larger” vol.  $O \sim 1 \text{ km}^3$ )*

*Reconstructed trajectory subset ( $\alpha, \beta = 10 - 40^\circ$ )*

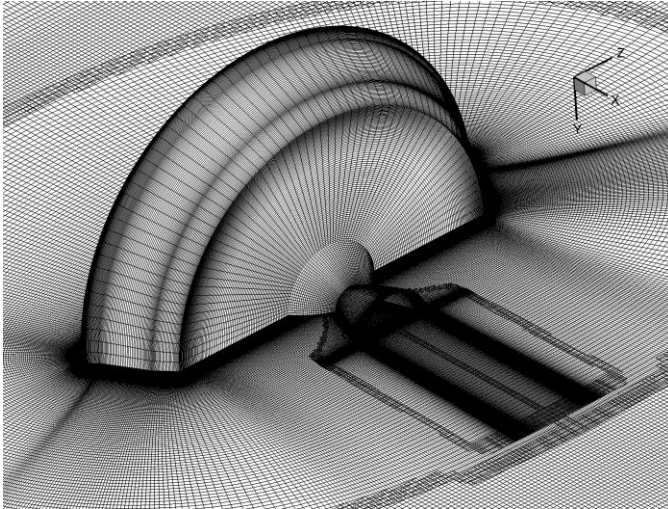
*Increase grid to accommodate  $\geq 40^\circ$  cases, seek grid convergence*



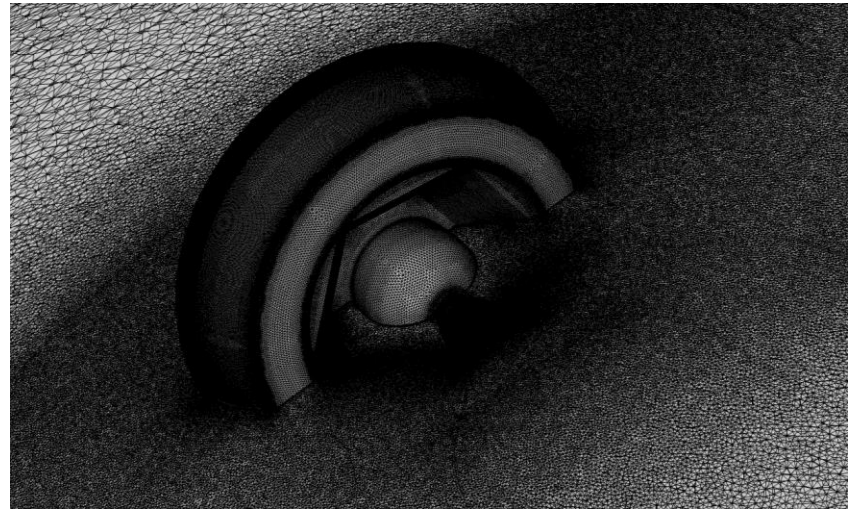


Aerodynamic Database 1.5

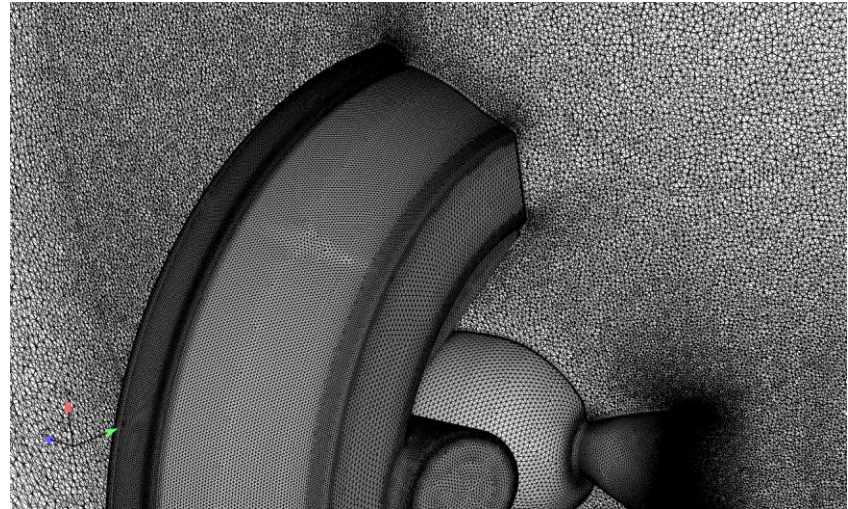
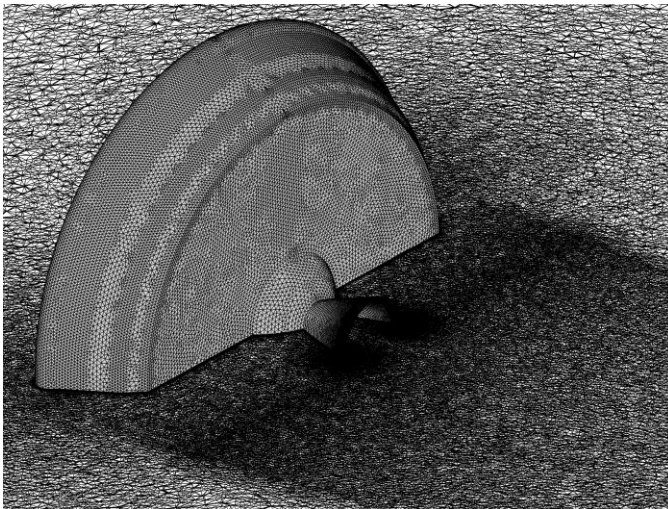
OVERFLOW



Loci-CHEM Runs (2015)

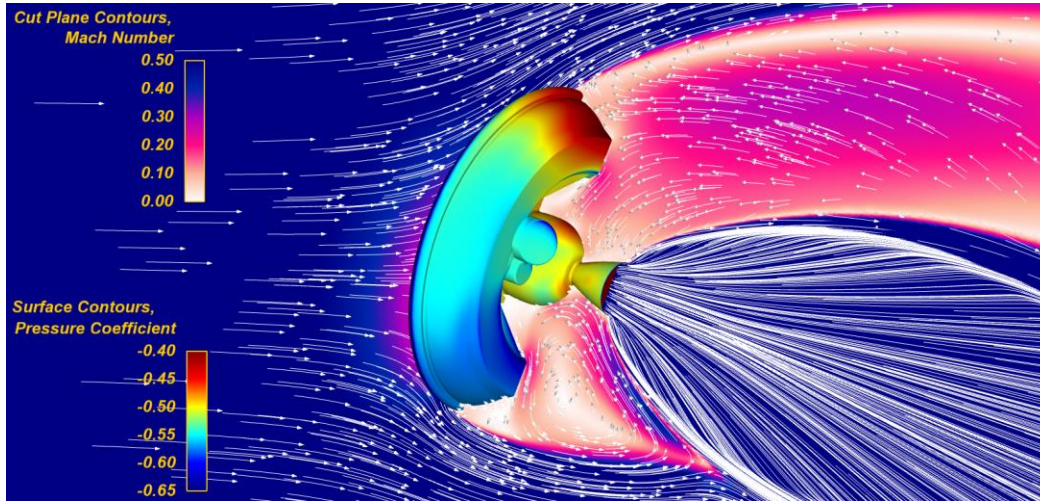


FUN3D

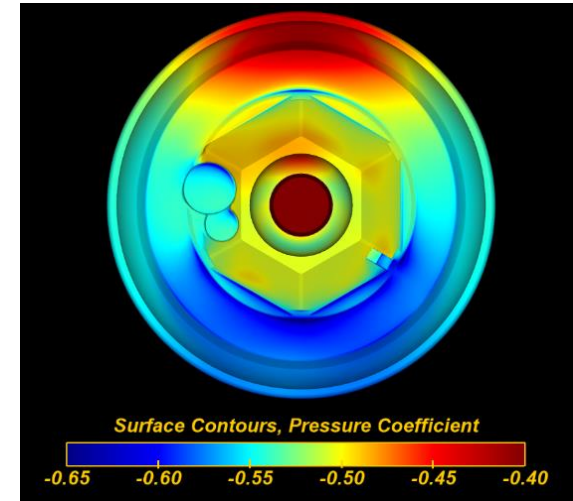




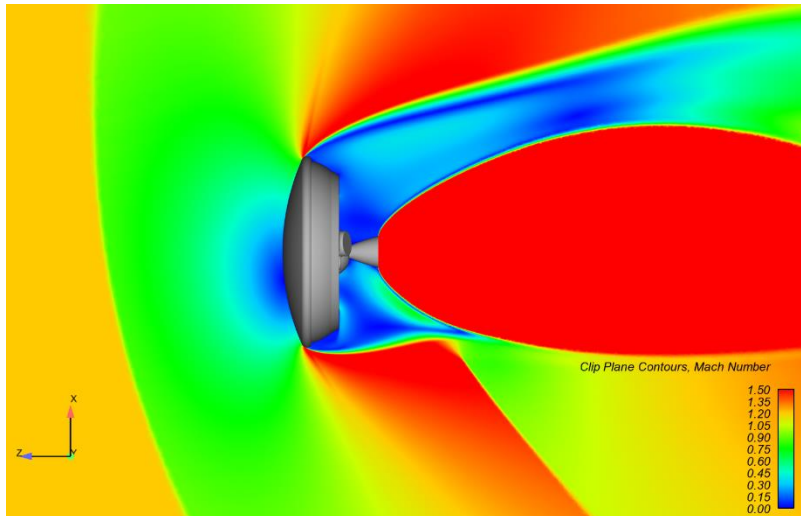
## STAR48 PLUME INDUCED AERODYNAMICS CFD, Mach = 0.7, Angle-of-Attack = 17.1°



## Base Pressure Coefficient

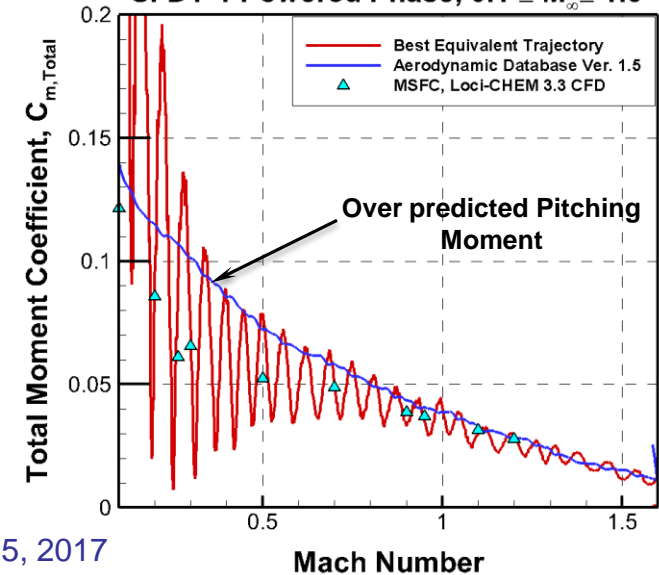


## CFD, Mach = 1.2, Angle-of-Attack = 11.5°

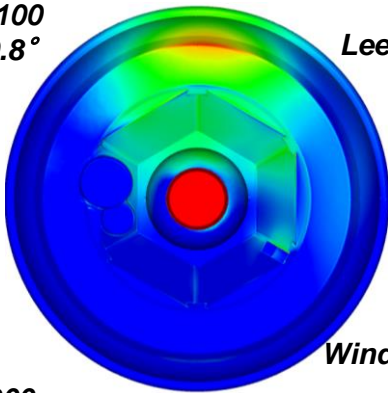


## SFDT-1 Lofting Impact

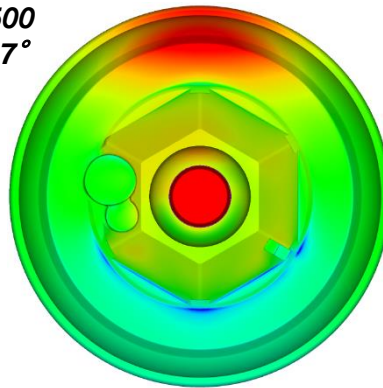
SFDT-1 Powered Phase,  $0.1 \leq M_{\infty} \leq 1.6$



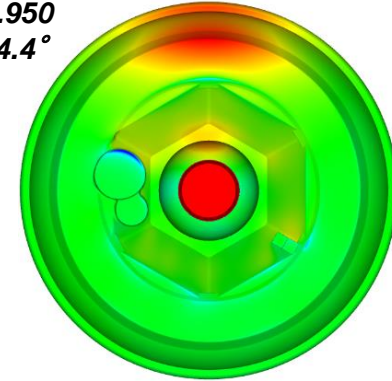
$M=0.100$   
 $\alpha = 40.8^\circ$



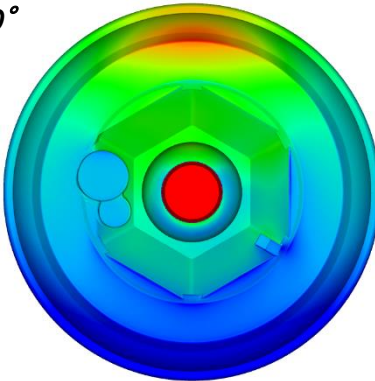
$M=0.500$   
 $\alpha = 17.7^\circ$



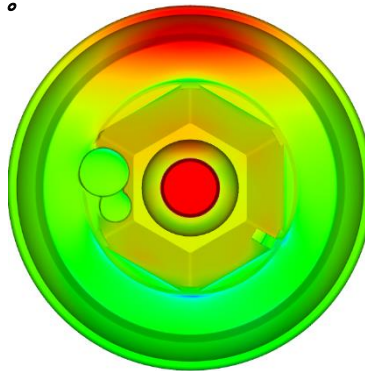
$M=0.950$   
 $\alpha = 14.4^\circ$



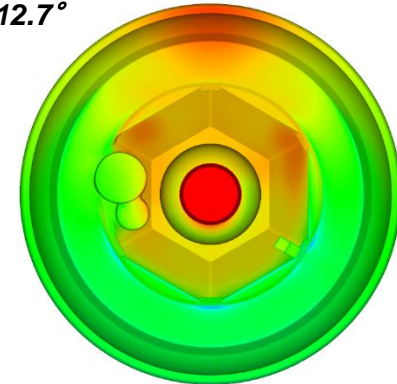
$M=0.200$   
 $\alpha = 30.0^\circ$



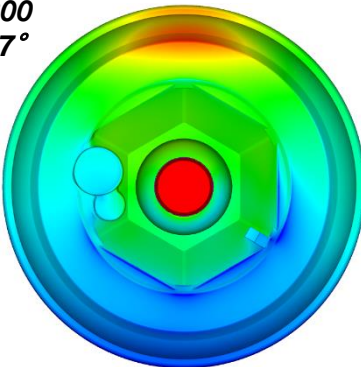
$M=0.700$   
 $\alpha = 17.1^\circ$



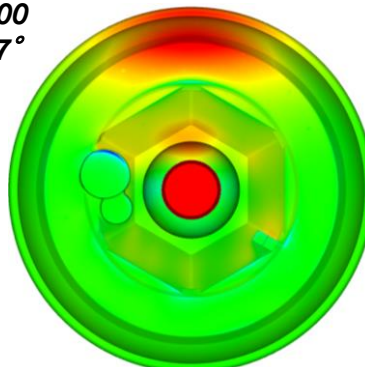
$M=1.10$   
 $\alpha = 12.7^\circ$



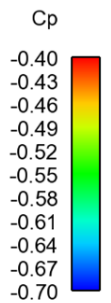
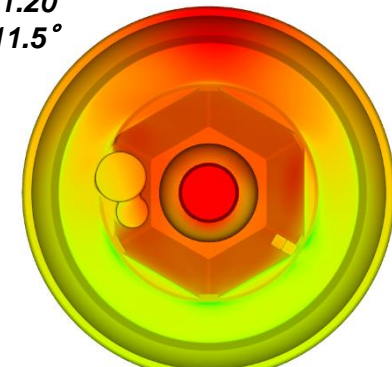
$M=0.300$   
 $\alpha = 14.7^\circ$



$M=0.900$   
 $\alpha = 14.7^\circ$



$M=1.20$   
 $\alpha = 11.5^\circ$

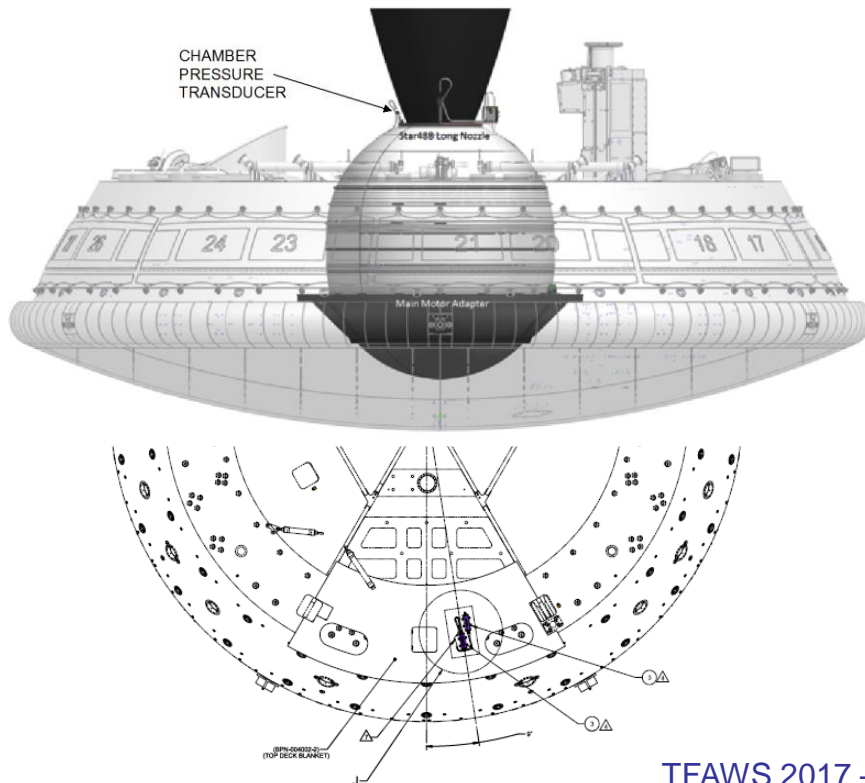




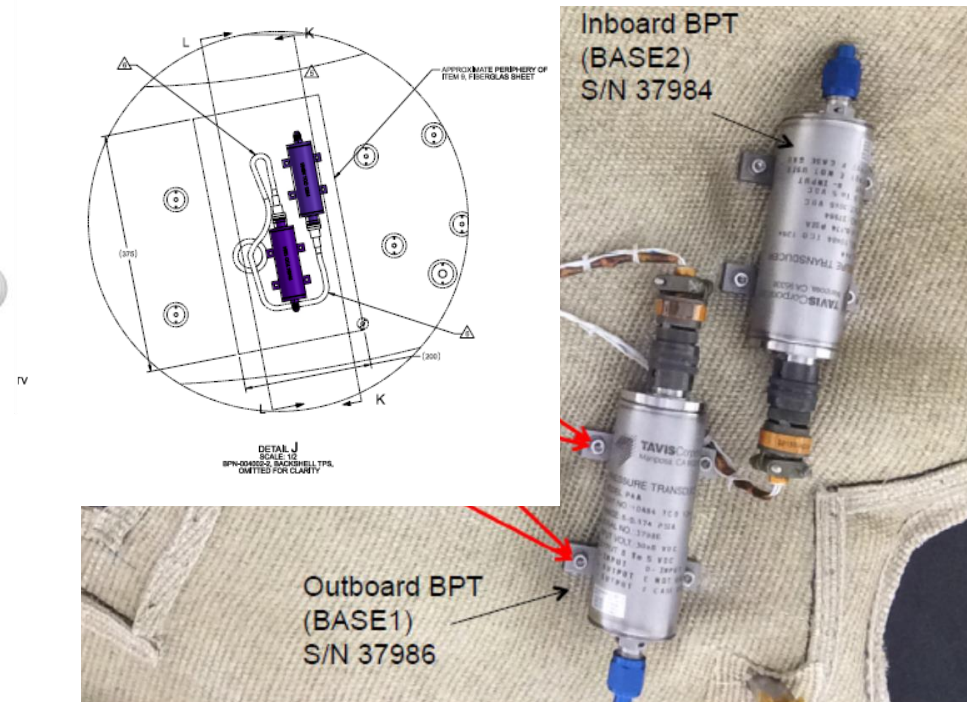
- Flight Instrumentation

- Star 48 chamber pressure, Kulite pressure transducer
  - Star 48 performance, thrust reconstruction
- Tavis (2) pressure transducers (0-0.137 psia)
  - Base pressure, aero model CFD validation

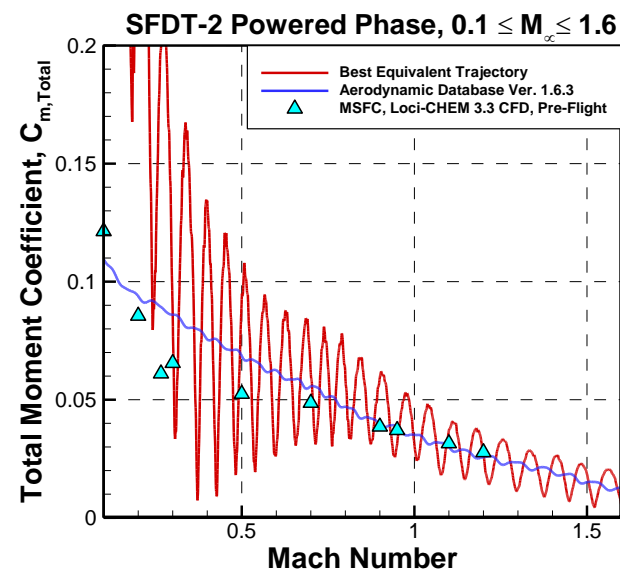
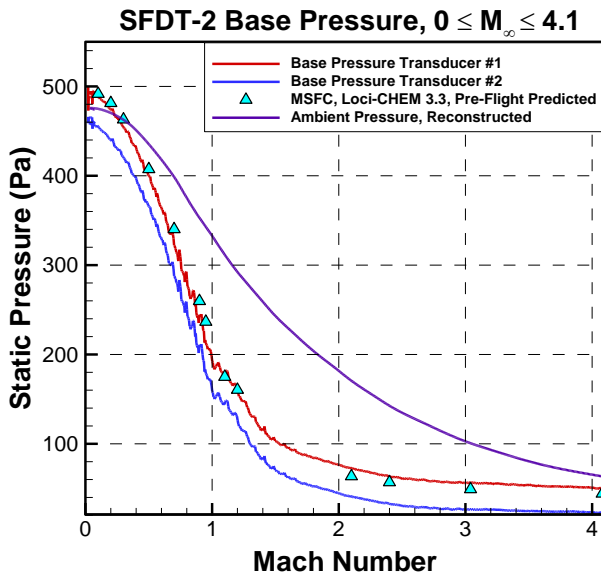
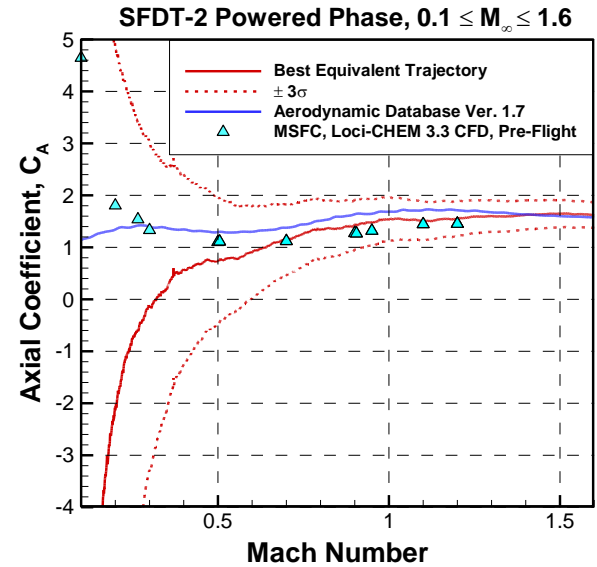
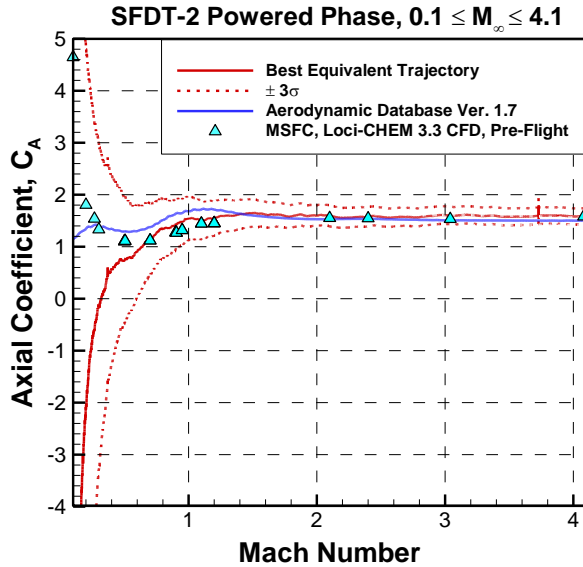
## Kulite pressure transducer



## Tavis pressure transducers

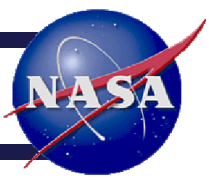








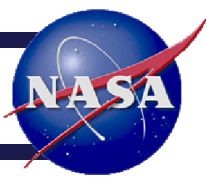
# Conclusions & Lessons Learned



- Plume induced environments - all thermal requirements met, robust thermal design validated, Star 48 power-on aerodynamic data base updated (ready for potent. SFDT-3)
- Highly under expanded plume-air interactions can be significant
  - Degree of expansion, plume size, can lead to a variety of consequences!
  - Observed similar plume induced environment issues with sep. motors
- Better understanding of the modelling sensitivities associated with single engine, plume induced base flow, in regards to the development of base eddy structure(s)
  - Cavity geometry provided greater base pressure recovery
  - Freestream BL separation point affected the point of impingement on Star 48 plume
  - Angle of attack, relative exposed plume area to the freestream
  - Match all nozzle exit conditions as best as possible

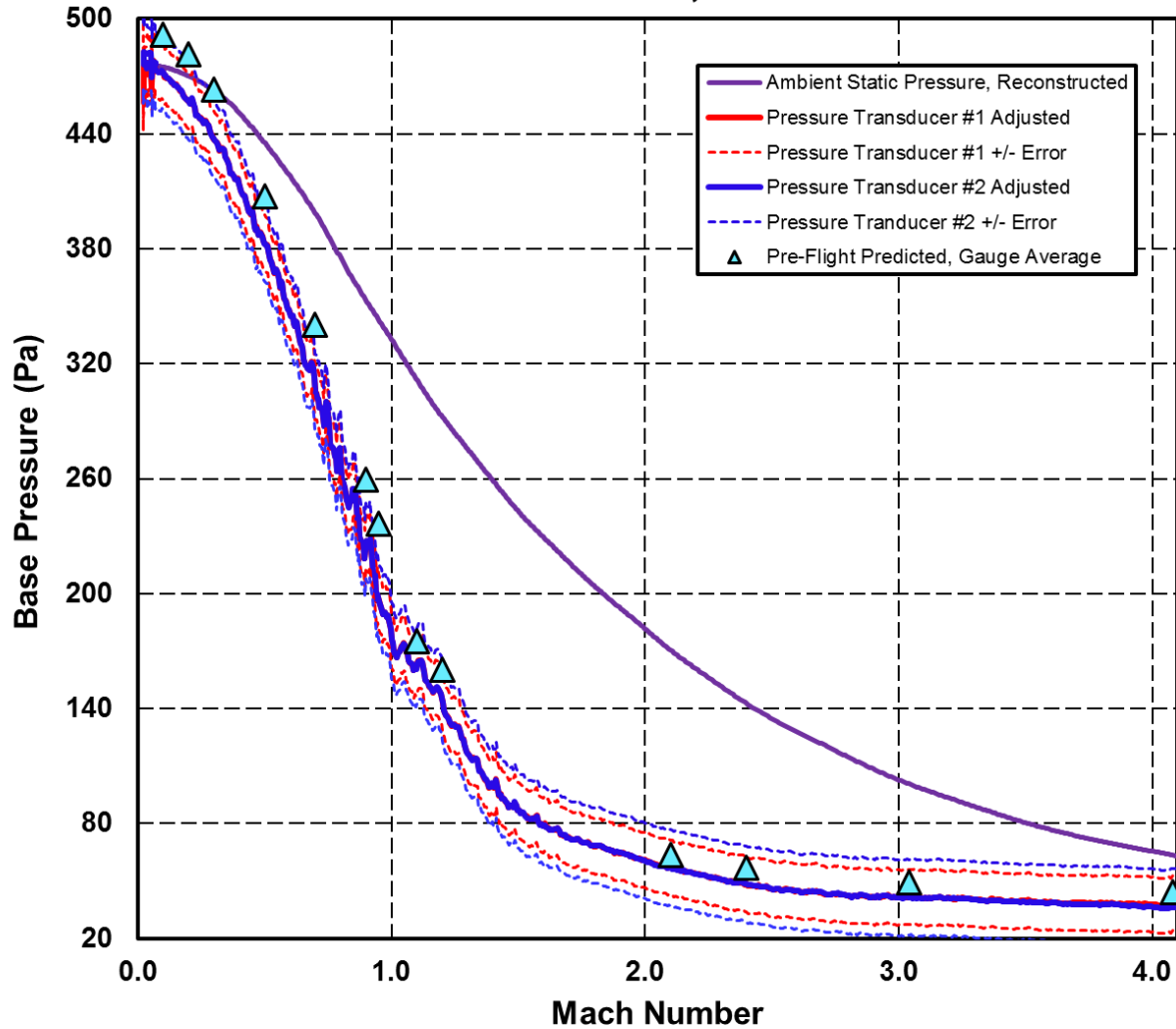


# Questions



Questions?

## SFDT-2 Base Pressure, Powered Phase





## Temperature Response

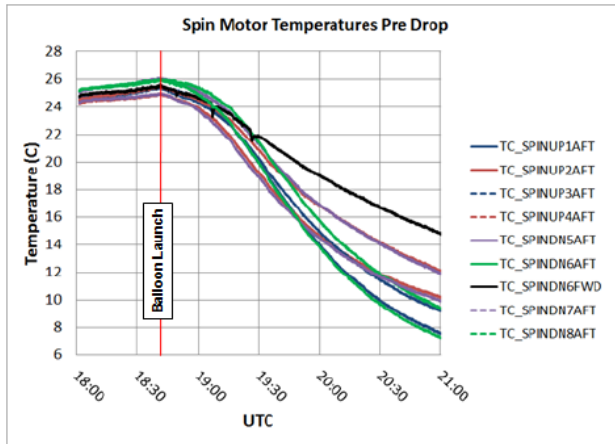


Figure 34. Spin Motor temperatures Pre Drop.

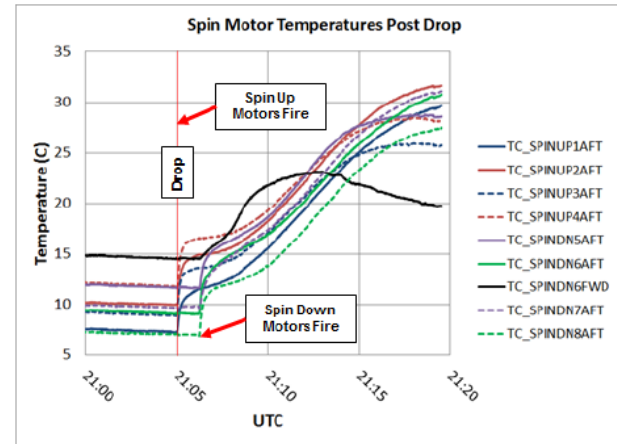


Figure 35. Spin Motor temperatures Post Drop.

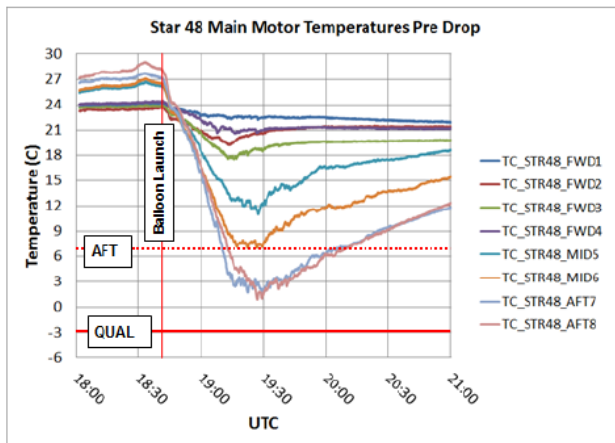


Figure 36. Star 48 Main Motor temperatures Pre Drop. AFT violation observed near nozzle during ascent.

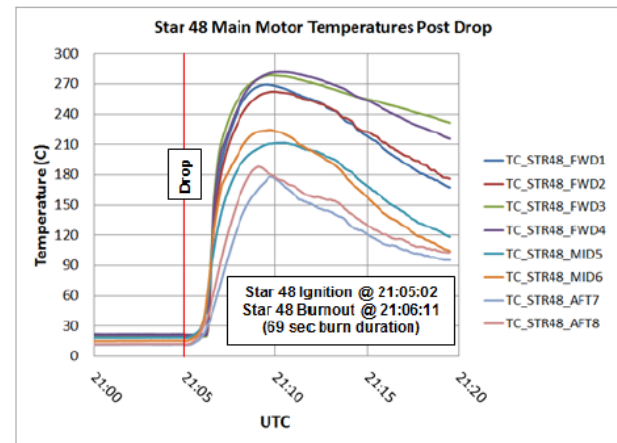


Figure 37. Star 48 Main Motor experienced soak back heating post engine burn up to a peak temp of 282°C.

## Temperature Response

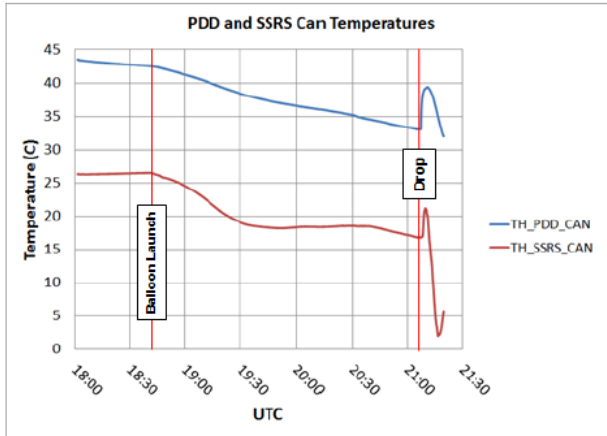


Figure 30. PDD and SSRS Canister temperatures. Inflation Aid within PDD canister likely at 44°C prior to deployment.

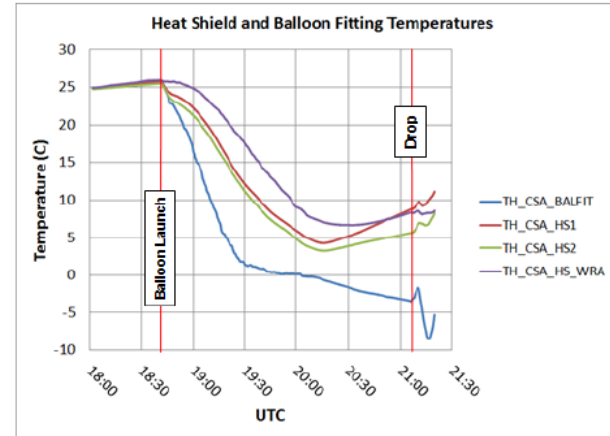


Figure 31. Heat Shield inner facesheet, Heat Shield Water Recovery Aid (WRA), and Balloon Fitting temperatures.

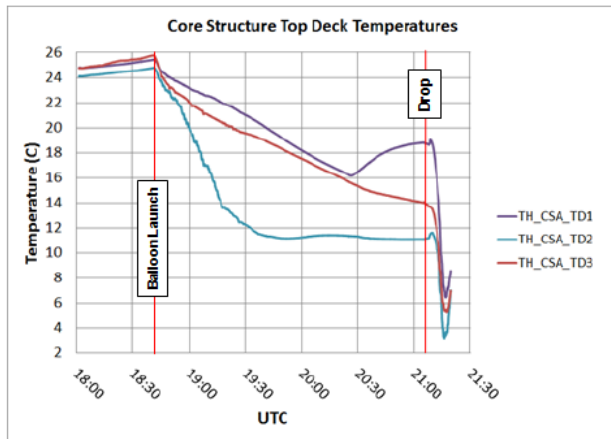


Figure 32. Core structure top deck outer facesheet temperatures.

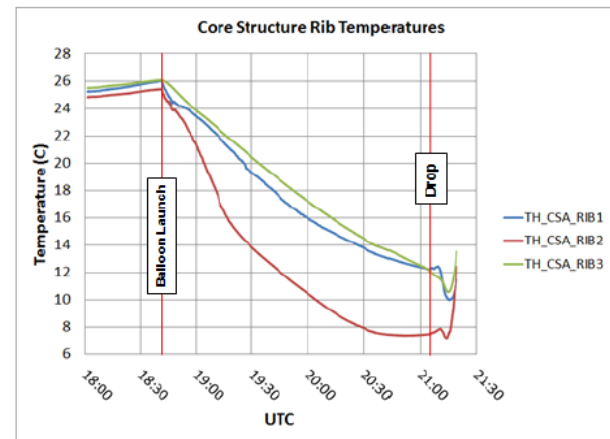
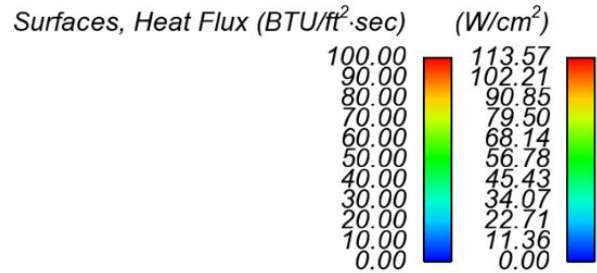
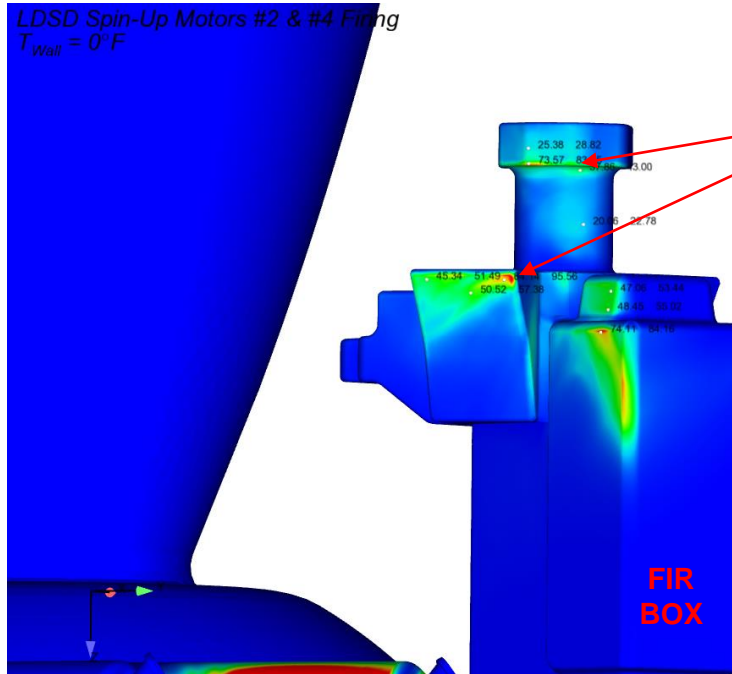
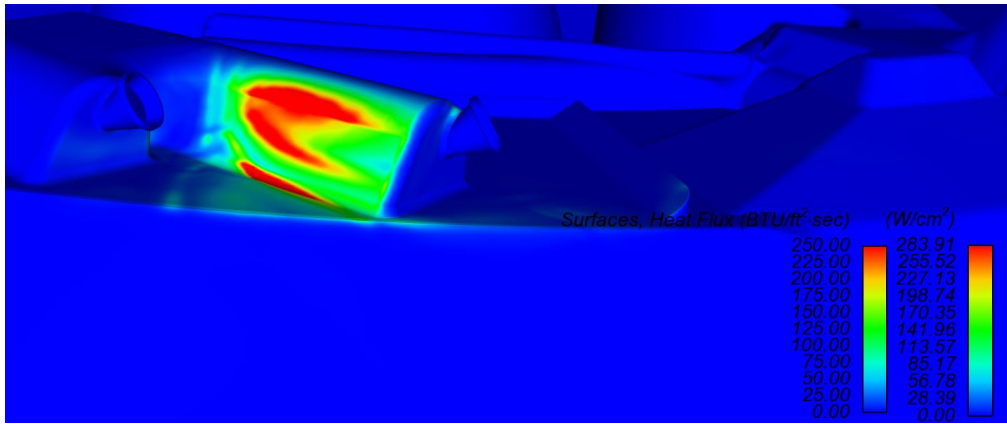


Figure 33. Core structure rib temperatures in vicinity of Star 48 Main Motor adaptor mounting ring.









# References

